Contract No.:

This manuscript has been authored by Battelle Savannah River Alliance (BSRA), LLC under Contract No. 89303321CEM000080 with the U.S. Department of Energy (DOE) Office of Environmental Management (EM).

Catalytic Effects of Silver in Iodine Reactors for Dissolved Used Nuclear Fuel

Jarrod. M. Gogolski[a]*, Kathryn. M. L. Taylor-Pashow[a], Tracy. S. Rudisill[a], Michael L. Restivo[a], John M. Pareizs[a], Robert. J. Lascola[a], Patrick E. O'Rourke[a], and William. E. Daniel[a]

[a]*Savannah River National Laboratory, Aiken, SC, USA*

*E-mail: jarrod.gogolski@srnl.doe.gov

Catalytic Effects of Silver in Iodine Reactors for Dissolved Used Nuclear Fuel

Dissolution of used nuclear fuel generates a variety of off-gasses including flammable hydrogen and other species which are a concern for environmental release. The H-Canyon facility at the Savannah River Site is currently dissolving aluminum-clad research reactor fuel from Material Test Reactors and the High Flux Isotope Reactor using a mercury-catalyzed nitric acid flowsheet. Savannah River National Laboratory recently developed and deployed a Raman spectrometer to monitor the off-gas stream from the dissolution process. Results from these measurements indicated a lack of the expected hydrogen, nitrous oxide, and nitric oxide in the off-gas stream. It was proposed that the silver on the silver nitrate-coated berl saddles present in the reactors for iodine capture were acting as a catalytic hydrogen recombiner. Nitric oxide is readily oxidized to nitrogen dioxide under normal conditions, but it was unclear what happened to the nitrous oxide. A laboratory scale iodine reactor was assembled and filled with silver nitrate-coated berl saddles to help ascertain the fate of nitrous oxide and hydrogen. Testing with this laboratory-scale reactor observed the recombination of hydrogen when a simulated dissolver off-gas was passed through the reactor containing silver nitrate-coated berl saddles at the approximate temperatures seen in H-Canyon. However, the nitrous oxide concentration was unchanged, suggesting a more complex process occurring within the off-gas stream before it reaches the iodine reactors at H-Canyon.

Keywords: Iodine Reaction, Hydrogen Recombination, NOx Gases

I. INTRODUCTION

The H-Canyon facility at the Savannah River Site (SRS) is dissolving aluminum-clad used nuclear fuel (UNF) from Material Test Reactors (MTR) and the High Flux Isotope Reactor (HFIR) at Oak Ridge National Laboratory. The UNF is dissolved using mercuric nitrate in nitric acid [1]. The uranium in the dissolved UNF is either purified for reuse or vitrified at the Defense Waste Processing Facility for long-term disposal as part of an ongoing effort to reduce the amount of UNF stored at SRS. The mercury-catalyzed dissolution process for the aluminum-clad, research reactor fuel in nitric acid [1, 2] results in a mixture of innocuous (e.g. N_2) and hazardous (e.g. H_2, NO_2, NO, and N_2O) off-gas species (collectively referred to as the off-gas stream). Reaction 1 shows an empirical equation that forms most of the gasses and has been previously determined by Hyder et al. to be representative of the conditions present in H-Canyon. Nitrogen dioxide, the other main gas, is formed as shown in Reaction 2 [3-5]:

$$Al + 3.75HNO_3 \xrightarrow{\text{catalyst}} Al(NO_3)_3 + 0.225NO + 0.15\ N_2O + 0.1125N_2 + 1.875H_2O \quad (1)$$

$$Al + 6HNO_3 \xrightarrow{\text{catalyst}} Al(NO_3)_3 + 3NO_2 + 3H_2O \quad (2)$$

The off-gas stream generated during the dissolution process passes first through a condenser, which serves to recover the nitric acid by converting the NO_x gases as shown in Reactions 3 and 4 [6]. It is then routed through a heated (173 to 188 °C) iodine reactor, which is packed with silver nitrate-coated berl saddles, to minimize the release of radioactive iodine to the environment, (Reaction 5) [6].

$$2NO + O_2 \rightarrow 2NO_2 \quad (3)$$

$$3NO_2 + H_2O \rightarrow 2HNO_3 + NO \quad (4)$$

$$6AgNO_3 + 3I_2 + 3H_2O \rightarrow 5AgI + AgIO_3 + 6HNO_3 \quad (5)$$

After leaving the iodine reactor, the off-gas stream passes through a particulate filter prior to being emitted from the stack. Savannah River National Laboratory (SRNL) recently started to monitor the off-gas stream of the UNF dissolutions using Raman spectroscopy [7], with the Raman spectrometer sampling point located after the particulate filter. The specific gases of interest are nitrous oxide (N_2O), nitric oxide (NO), nitrogen dioxide (NO_2), hydrogen (H_2), water (H_2O), nitrogen (N_2), and oxygen (O_2). Monitoring the off-gas stream will help determine if the UNF dissolution is complete prior to reaching the end of the scheduled dissolution time. Shorter dissolution times are desired to increase the H-Canyon throughput for UNF.

Development and testing of the Raman spectrometer during the dissolution of MTR and HFIR fuels using the mercury-catalyzed nitric acid flowsheet showed that N_2O, NO, and H_2 were not detected in the off-gas stream. The absence of these gases indicates that other side reactions are occurring, with one potential location being within the iodine reactor. A lab-scale iodine reactor was built, and then tested with a simulated off-gas stream to help elucidate the disappearance of N_2O and H_2. Previous studies noted that silver can be used for catalytic hydrogenation [8-10], Reaction 6. However, the catalytic conditions within the iodine reactor are not conducive to N_2O reduction [11], so it is unclear what is causing the disappearance of the N_2O from the off-gas stream of the dissolved UNF.

$$H_2 + \tfrac{1}{2}O_2 \xrightarrow{Ag^+} H_2O \quad (6)$$

Separately, while NO is a significant component from the dissolution of MTR fuel, when exposed to an air purge it would convert to NO_2 and therefore would not be observed at the Raman spectrometer sampling point [2]. Accurate analysis of NO would have required an oxygen deprived environment [12], which would have interfered with the potential reaction of interest (Reaction 6).

Data from previous laboratory dissolution experiments to define the MTR flowsheet were used to examine the range of off-gas compositions seen in a typical dissolution [1]. These laboratory-scale experiments measured the off-gas composition and generation rates during dissolution of Al 1100 alloy coupons. This data was then scaled to determine off-gas generation rates for the dissolution of typical bundles of research reactor fuels in H-Canyon. As the composition of the dissolver off-gas stream changes throughout the dissolution, a range of compositions with varying H_2 concentrations were selected for testing.

II. METHODS AND MATERIALS

II.A Preparation of Silver Coated Berl Saddles

Unglazed porcelain berl saddles (obtained from Chemglass Life Sciences) with an outer diameter of 8 mm were coated with silver nitrate ($AgNO_3$, 99.9% purity from Alfa Aesar) using the following procedure. A batch of berl saddles (~29 g) was immersed in a 13 – 14 M $AgNO_3$ solution for three minutes at 82 °C with constant mixing. The berl saddles were contained in a perforated borosilicate glass basket fabricated by the SRNL Glass Shop. Solution density was periodically checked (desired range of 2.2 – 2.4 g/mL [13, 14]) and adjusted as needed with either additional deionized (DI) water or $AgNO_3$. After removal of the berl saddles from solution, they were rinsed with DI water to remove excess $AgNO_3$. The berl saddles were air dried before being dried in an electric oven at 121 °C for six hours. A summary of the weight percent (wt. %) gains for each batch of dried silver nitrate-coated berl saddles is provided in Supplemental Table SI. The average weight increase was 11.3 wt. %. The silver nitrate-coated berl saddles were slightly darker than the uncoated berl saddles (Figure 1). The lack of a drastic color change, considering a 11.3% average mass increase, indicated that the $AgNO_3$ in solution was able to permeate the porous berl saddles to make a uniform $AgNO_3$ coating. While previous studies reported that a 5.0 wt %

increase was expected, [15] those studies were also coating significantly larger batches of berl saddles. This would suggest that other factors (temperature, solution volume, and submersion duration) significantly impact the amount of $AgNO_3$ deposited on the berl saddles.

Figure 1: Photograph of uncoated berl saddles (left) and silver nitrate coated berl saddles (right).

II.B Laboratory Scale Iodine Reactor and Gas System

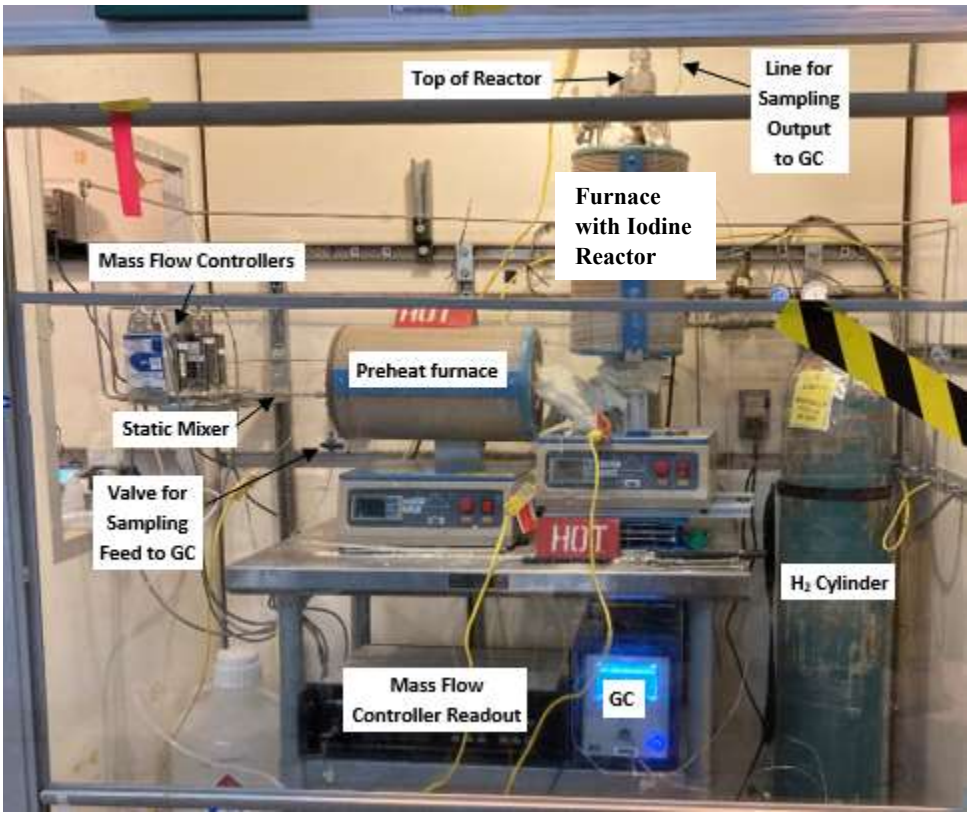

Figure 2. Photograph of laboratory scale apparatus (Gas cylinders for NO, N_2O, and NO_2 are not shown.)

The laboratory scale equipment modeling the gas flow through the H-Canyon Iodine Reactor was assembled in the Engineering Development Lab of the SRNL (Figure 2 and Supplementary Figure S1). A data acquisition and control system with the software Labview by NI™, Version 2014 was used to control and record gas flow rates with mass flow controllers and record thermocouple readings. All gas flows were set and monitored using MKS mass flow controllers and stainless-steel tubing was used for the gas lines. A Micro GC (gas chromatograph) Fusion® Gas Analyzer was used to measure the concentration of the gasses in the simulated off-gas stream both upstream (feed) and downstream of the reactor. The gas chromatogram using a Molsieve 5A column (Channel A) was used to quantify H_2 and O_2 (plotted in Figure 3A) and a Q-Bond column (Channel B) for quantification of N_2O (plotted in Figure 3B). Both channels used a thermal conductivity detector. Calibration gas streams (Mesa Specialty Gases & Equipment) contained a mixture of H_2, N_2O, and either air or N_2. The area under the H_2, N_2O, and O_2 peaks were used for constructing the vol. % calibration curve for the respective gases. (A closing calibration check was also done each day with one calibration gas, and the results were always within 5% of the value obtained at the start of the day.) Each GC measurement was a total of seven, 2-minute runs, and the last five results were averaged to obtain a single average value for each set of conditions. Experiments used either uncoated or silver nitrate-coated berl saddles packed into the reactor.

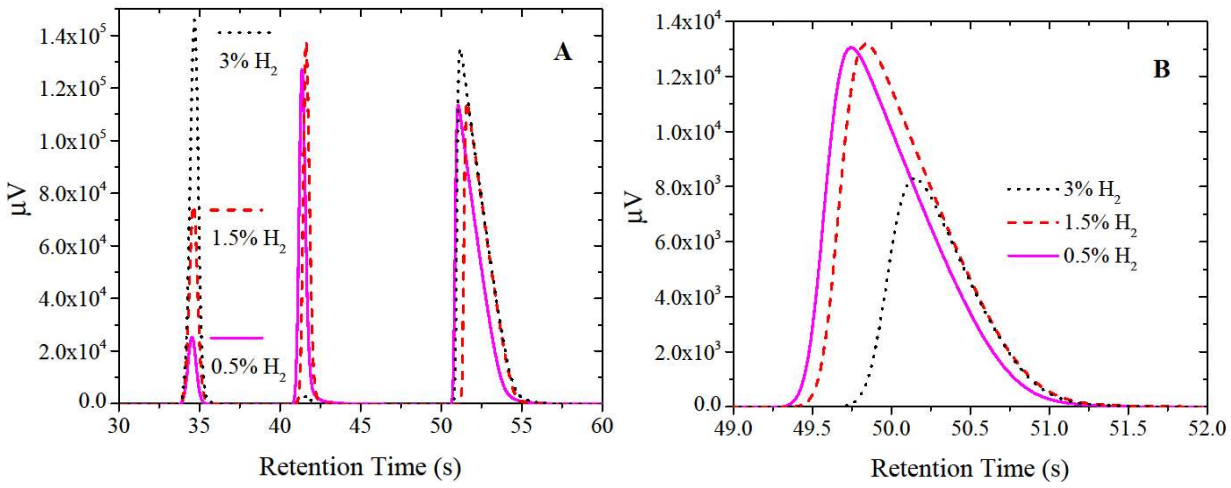

Figure 3: Chromatogram of calibration gases on Column A (A) and on Column B (B), note the balance gas for 3.0% H_2 was pure N_2 vs. air used in the 0.5% and 1.5% H_2 calibration gases. The retention time for both columns was taken from 0 – 88 s, but the full scale was truncated for clarity. Column A shows H_2 (34 s), O_2 (41 s), and N_2 (~52 s). Column B shows N_2O (~50 s).

The individual gases were mixed using an inline Koflo Model PN ¼-21 static mixer before entering the first furnace. The reactor was fabricated from stainless steel tubing with a nominal inside diameter of 3.12 cm. The total length of the reactor was 45.72 cm (interior dimension); however, the bed length (packed with berl saddles) was nominally 20.32 cm. A photograph of the reactor vessel is shown in Figure 4. A stainless-steel insert was used to position the start of the bed approximately 17.70 cm above the bottom of the tube. Four Type-K thermocouples were used to monitor temperatures at the following locations: prior to entering the first furnace (after the static mixer); between the first and second furnaces; in the berl saddle reactor bed (set to 173 – 188 °C); and upon exiting the reactor.

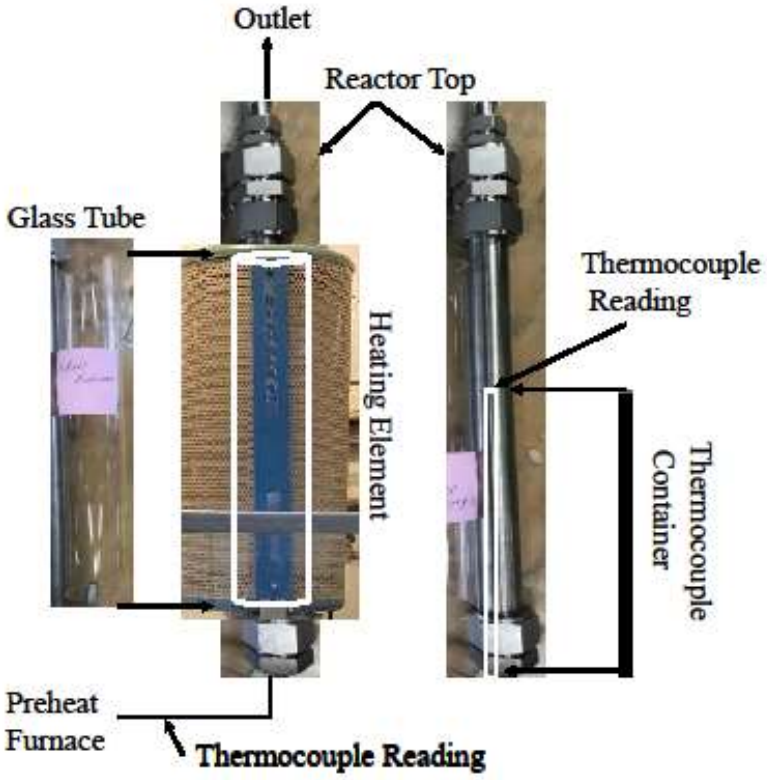

Figure 4: A closeup of the lab scale iodine reactor and position within heating element from Figure 2, the adjacent glass tube was used to ensure there was no contact with the heating elements while the reactor was in the furnace. Thermocouple readings of the simulated offgas between the two furnaces and approximately halfway in the reactor (in the berl saddle bed) are illustrated.

Table I: Feed Composition of Off-Gas Stream

Experiment	H_2	NO	N_2O	Air
#	Vol %			
1	1.0	16.6	5.2	77.2
2	1.9	22.3	11.0	64.8
3	2.8	32.6	13.6	51.0
4	1.0	0	0	99.0
5	1.9	0	0	98.1

Previous laboratory-scale aluminum dissolution studies [1, 2] were examined to determine the expected range of H_2, NO, N_2O, and Air gas concentrations from H-Canyon dissolutions, which were bounded by the test matrix defined in Table I**.** Table I is therefore a summary of the feed composition test matrix used for the following experiments. The feed composition for Experiment #1 represents the stage in the dissolution where the aluminum concentration is 0.03 M and the composition shown for Experiment #2 represents the point in the dissolution when the aluminum concentration is 0.09 M. Experiment #3 is the point in the dissolution where the maximum off-gas rate was determined to occur (aluminum concentration of 0.16 M). The off-gas stream also contains small amounts of NO_2; however, due to the low concentrations (<1%), it was excluded from this testing to simplify the feed composition. The amount of NO_2 in each case was replaced with additional NO. Small amounts of oxygen and nitrogen are also produced in the off-gas stream, but the amounts are small relative to the air purge, and therefore these amounts were replaced with additional air. Experiments #4 and #5 were designed to determine if NO and N_2O have any impact on the recombination reaction of hydrogen. The air stream contains approximately 19% O_2, 80% N_2, with trace amounts of other gases, and H_2O vapor (due to the humidity).

The residence time (t_r) of the off-gas stream in the laboratory-scale iodine reactor was matched to the residence time for the H-Canyon iodine reactor to properly reflect the amount of time the off-gas stream is in contact with the berl saddles within the iodine reactor (see Supplemental Information). A summary of the results is provided in Table II. In addition, the residence times were varied from 0.5x to approximately 5x of the calculated residence time within the limits of achievable gas flows with the mass flow controllers used. (Supplemental Tables SII – SVII are summaries of full test matrixes and experimental conditions used.)

Table II: Calculated Off-Gas Residence Times

% H_2 of Total Off-Gas	Max. Off-Gas from System (m^3/min)		Off-Gas t_r in Bed (s)
	at 15.5 °C, 1 atm	at 200 °C, 1 atm	
1.0	1.49	2.45	10
1.9	1.82	2.98	8
2.8	2.28	3.73	7

III. RESULTS AND DISCUSSION

III.A Analysis of H_2 in Simulated Off-Gas Stream

A summary of the results using the simulated dissolver off-gas streams with both the uncoated and silver nitrate coated berl saddles are provided in Table III. As can be seen in each set of experiments with the uncoated berl saddles, the measured H_2 concentration in the output stream was the same (within 5%) as the input. The cause for the consistent slight increase in H_2 (from the input to output sampling points) is uncertain but this shows that H_2 does not recombine or otherwise react in the reactor bed in the absence of the silver catalyst. In contrast, in experiments with the silver-coated berl saddles, the H_2 concentrations measured in the output streams were significantly reduced ($\geq$ 90%). Most of the measured output H_2 concentrations in tests with the silver-coated berl saddles were below the concentration of the lowest standard (0.5%), requiring extrapolation of the calibration curve.

Table III. Measured H_2, O_2, and N_2O concentrations in experiments 1 – 5.

Test ID	t_r	H_2		O_2		N_2O		H_2 Recombination
		Input	Output	Input	Output	Input	Output	
	(s)	Vol%						%
1A-UC	10.3	1.03	1.07	8.66	8.55	5.85	5.89	-3.42
1A-C	10.3	1.03	0.013	8.39	8.15	5.93	6.09	98.8
1B-C	20.6	1.07	0.012	9.28	8.67	5.96	6.09	98.9
1C-UC	48.9	0.943	0.943	11.00	10.71	4.89	4.90	0.04
1C-C	48.9	1.02	0.011	10.35	9.29	5.76	5.98	98.9
1D-C	5.14	1.02	0.102	9.03	8.71	5.80	5.80	90.0
2A-UC	8.44	2.00	2.03	4.54	4.02	12.4	12.4	-1.90
2A-C	8.44	1.99	0.065	4.28	3.29	12.6	12.9	96.7
2B-C	16.9	2.07	0.018	4.11	2.86	13.1	13.6	99.1
2C-UC	40.9	1.88	1.97	6.35	5.52	11.5	12.1	-5.01
2C-C	40.9	1.97	0.016	5.49	4.07	12.1	12.8	99.2
3A-UC	10.1	3.05	3.04	0.07	0	16.7	16.4	0.27
3A-C	10.1	2.98	0.061	0.07	0	16.4	16.3	97.9
3B-UC	32.0	2.99	3.07	0.46	0	16.0	16.7	-2.84
3B-C	32.0	2.96	0.024	0.24	0	15.5	15.9	99.2
4A-C	10.3	0.971	0.020	20.04	19.95	N/A	N/A	97.9
4B-C	20.6	0.968	0.003	19.99	19.88	N/A	N/A	99.7
4C-C	51.4	1.043	0.001	19.97	19.99	N/A	N/A	99.9
4D-C	5.14	0.964	0.091	20.17	19.99	N/A	N/A	90.6
5A-C	8.44	1.79	0.060	19.97	19.82	N/A	N/A	96.7
5B-C	16.9	1.85	0.011	20.02	19.85	N/A	N/A	99.4
5C-C	42.2	1.76	0.002	20.01	19.79	N/A	N/A	99.9

*The Test ID denotes experiment # (from Table I), the varying residence times are denoted by A (1x), B (2x), C (~ 4.75x), D (0.5x), and silver deposition on the berl saddles U = uncoated, C = silver-coated.

Figure 5 illustrates the effect of the increasing residence time on the recombination reaction. At the shortest residence times (t_r = ~ 5 s), which represents half of the expected residence time for the 1.0% H_2 condition, the percent recombination is still approximately 90%. A condition observed regardless if there are NO_x gasses in the simulated off-gas stream. (The effects from the addition of NO_x gases are elaborated in the following section.) However, the H_2 recombination increases significantly (96.7%) at t_r = 8.4 s; and is 97.9% or greater for all residence times over ten seconds. No correlation was found between the starting H_2 concentration and the extent of

recombination. An example of the raw GC spectra obtained for experiments 1C-C and 1D-C (4.75x vs. 0.5x t_r) is provided in Figure 6. The contrasting GC spectra for H_2 illustrates the disappearance of H_2 in the outlet stream after passing over the silver catalyst and its similarity to an air stream.

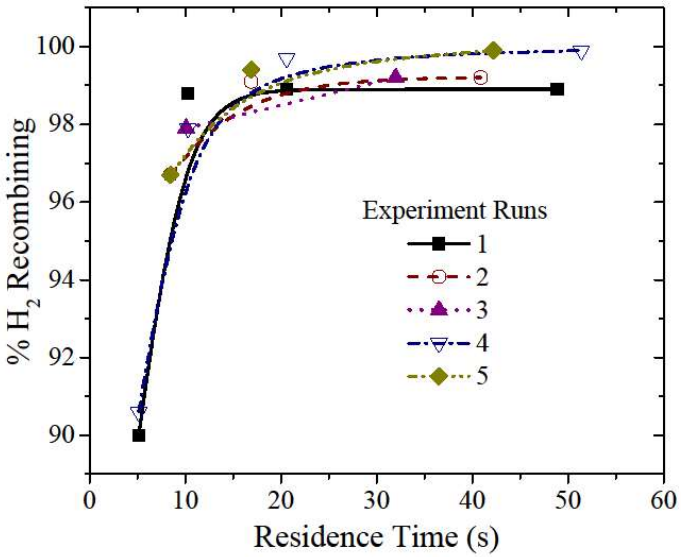

Figure 5. Effect of residence time in reactor on the H_2 recombination. A graphical representation of silver-coated berl saddle experiments from Table III.

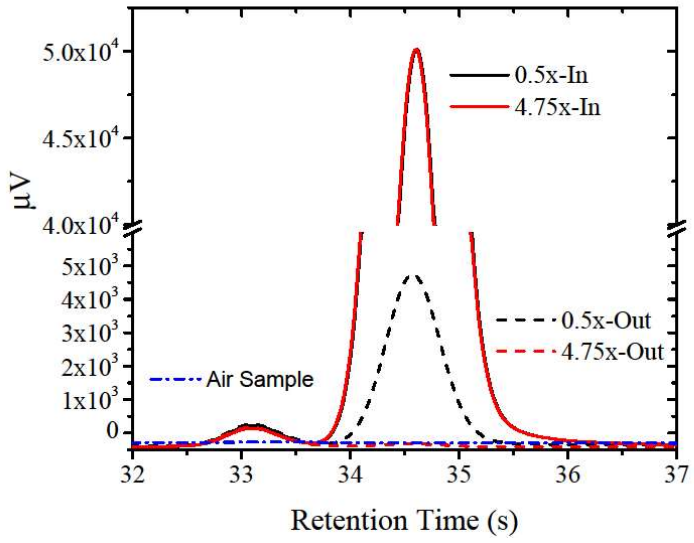

Figure 6. Comparison of GC spectra (Module A) of H_2 for experiments 1A-C and 1C-C (0.5x vs. 4.75x residence times) with an air sample as a reference.

III.B Analysis of NO_x in Simulated Off-Gas Stream

Comparing experiments 1 with 4 and 2 with 5 (Table III) shows that there is not a consistent trend with the presence or absence of the NO and N_2O gases impacting the H_2 recombination reaction. For the 1.0% H_2 feed (experiments 1 and 4), it does appear the recombination is slightly higher in the absence of the NO and N_2O gases, except at t_r =1x. Similar results are also seen for the 1.9% H_2 feed (experiments 2 and 5). Considering the low H_2 concentrations being measured, these differences are likely within the analytical uncertainty of the measurements. The observed vol. % of N_2O, also reported in Table III and illustrated in Figure 7, shows that there are no significant changes in N_2O concentration after passing through the reactor at various residence times. The peaks show both the characteristic shift and transition from a symmetrical peak to a sharper angle for N_2O.

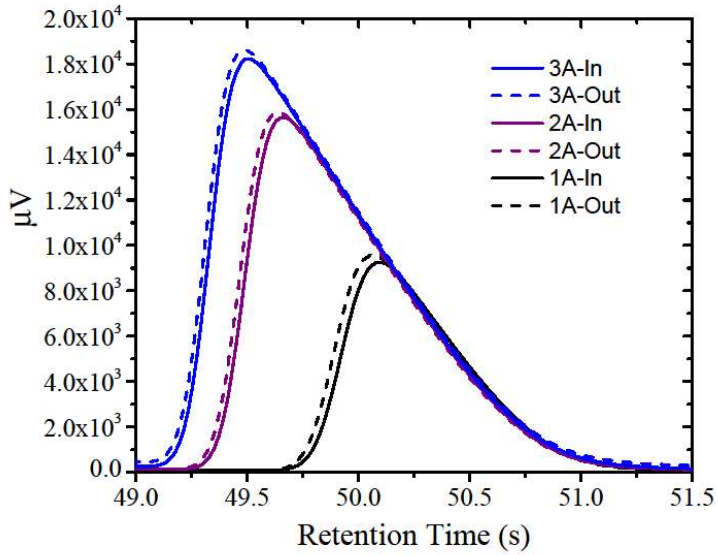

Figure 7: Comparison of input and output GC spectra (Module B) of N_2O for experiments 1A, 2A, and 3A with silver coated berl saddles.

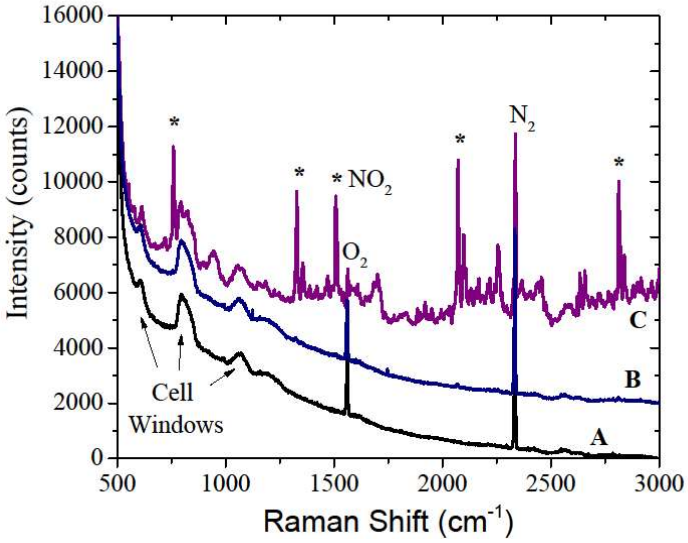

Figure 8: 640 nm Raman spectra showing No Steam (A), End of Dissolution with 0.13% NO_2 (B), Peak Emission with 6% NO_2 (C). The five lines denoted by asterisks were used to quantitate NO_2. Spectra are offset for clarity.

The unchanged vol. % of N_2O is peculiar because N_2O would not have been recovered within the condenser step during the UNF dissolution process [11] nor would have thermally decomposed under the conditions in this experiment [16]. Yet, the analysis from the H-Canyon Raman spectrometer did not report any N_2O after the iodine reactor. Figure 8 shows Raman spectra of dissolver off-gas obtained at three points of processing: when the steam is off (i.e., before heating the dissolver), during the peak of the emission, and near the end of the dissolution. The spectra before and at the end of processing are essentially of air (N_2 at 2331 cm^{-1} and O_2 at 1556 cm^{-1}), with trace amounts of NO_2 present at the end. The NO_2 measurements and the rate of change of those measurements can be correlated with the small amount of gas generated at the tail end of the dissolution, when there is only a fraction of the charged material remaining to be dissolved. There are several background peaks that are due to Raman scattering from the cell windows that fortunately do not interfere with any of the analytically sensitive lines. The spectrum at the peak

of the dissolution shows a multitude of additional lines but these are also entirely due to NO_2 (asterisks in Figure 8 denote the most analytically useful peaks, approximately 751, 1321, 1501, 2065, and 2808 cm^{-1}). A band due to H_2O is seen at ~1650 cm^{-1}. The most prominent peaks for N_2O (1284 and 2222 cm^{-1}), NO (1876 cm^{-1}), and H_2 (352, 586, 813, and 1034 cm^{-1}) were not observed. The estimated limits of detection for these species are 0.37%, 2.5%, and 0.61% respectively; the dilution factor associated with the air purge in the dissolver tank is not known.

The N_2O could be decomposing either from radiolysis or reacting with electronically excited N_2 or N radicals into N_2 and O_2 before reaching the Raman spectrometer sampling point [17, 18]. Although, it is unlikely that radiolysis would account for the complete decomposition of N_2O since the N_2O gas can quickly leave the dissolver solution where the radiation field is the highest. The cause for the disappearance of N_2O remains unclear [7].

III.C Analysis of O_2 in Simulated Off-Gas Stream

Table III shows that the observed O_2 vol % drops as it passes through the lab scale iodine reactor. It is important to note that previous studies observed that O_2 is readily absorbed onto the metallic silver [8], which means O_2 can accumulate on the silver coated berl saddles. While the O_2 consumed in all available reactions (e.g., H_2 recombination, oxidation of NO, etc.) cannot be accurately quantified, the general trend that the concentration of O_2 drops was observed. The average O_2 vol % drop is highest for the gas stream including NO_x gases passing over the silver coated berl saddles, then the NO_x containing stream passing over the uncoated berl saddles, and the lowest drop observed for the gas stream without any NO_x gases passing through the silver coated berl saddles. This trend directly correlates to the additional opportunities for O_2 to react. Raman spectra of the off-gas during H-Canyon dissolver runs also indicated that the concentration ratio of O_2 to N_2 decreased during peak dissolving conditions compared to the expected ratio

observed before and at the end of a dissolver run. This is consistent with the consumption of O_2 gas during NO_x oxidation as well as the production of N_2 as part of the dissolution (Reaction 1).

IV. CONCLUSIONS

It is likely that the lack of H_2 observed in the Raman spectroscopic analysis of the H-Canyon dissolver off-gas during UNF dissolution in nitric acid is due to the dissolver off-gas stream passing through the silver nitrate-coated berl saddles in the iodine reactor. Also, control experiments with uncoated berl saddles resulted in no change to the hydrogen concentration after passing through the reactor. The residence time of the gas in the reactor was varied to determine if residence time had an impact on the amount of hydrogen recombination occurring. Results from these experiments indicated at the shortest residence times tested (~5 s) recombination of the hydrogen still exceeded 90%; however, the percent recombination did increase at longer residence times, reaching 97.9% or greater for residence times over 10 seconds. Finally, testing with a simplified off-gas composition containing only H_2 and air gave similar results, indicating that the presence of NO and N_2O gases in the off-gas stream do not play a role in the recombination reaction.

Gas chromatography was selected for this work as the focus was on hydrogen; however, since the Raman spectrometer installed to monitor the H-Canyon off-gas is only detecting NO_2, it would be beneficial to do similar measurements on the lab scale set-up to ascertain the fate of the NO. Raman spectroscopy measurements can confirm that the NO is quickly oxidized to NO_2 in the presence of oxygen. Additional sampling points for the Raman spectrometer on the H-Canyon off-gas system, such as a point prior to the iodine reactor, would help determine what is occurring with the N_2O.

V. ACKNOWLEDGEMENTS

This work was supported by Savannah River Nuclear Solutions, Environmental Management Operations. This work was also produced by Battelle Savannah River Alliance, LLC under Contract No. 89303321CEM000080 with the U.S. Department of Energy. Publisher acknowledges the U.S. Government license to provide public access under the DOE Public Access Plan (http://energy.gov/downloads/doe-public-access-plan).

VI. DECLARATATION OF INTEREST

The authors report there are no competing interests to declare.

References:

[1] Daniel, W. E., Rudisil, T. S., & O'Rourke, P. E. (2018). *Dissolution of material test reactor fuel in an H-Canyon Dissolver* (SRNL-STI-2016-00725). Savannah River National Laboratory

[2] Daniel, W. E., Rudisil, T. S., O'Rourke, P. E., & Karay, N. S. (2017). *Dissolution flowsheet for high flux isotope reactor fuel* (SRNL-STI-00485). Savannah River National Laboratory

[3] Almond, P. M., Daniel, W. E., & Rudisil, T. S. (2015). Dissolution and off-gas results for U-Al and Al alloys representative of MURR-Type used nuclear fuels. *Separation Science and Technology, 50*, 2790-2797.

[4] Wymer, R. G., & Blanco, R. E. (1957). Uranium-aluminum alloy dissolution. *Industrial and Engineering Chemistry Research: ACS Publications, 49*(1), 59-61.

[5] Caracciolo, V. P. (1959). *Dissolver for uranium-aluminum alloy tubes* (DP-398). E. I. du Pont de Nemours and Company, Savannah River Laboratory

[6] Hyder, M. L., Perkins, W. C., Thompson, M. C., Burney, G. A., Russel, E. R., Holcomb, H. P., & Landon, L. F. (1979). *Processing of irradiated, enriched uranium fuels at the Savannah River Plant* (DP-1500). Savannah River Site

[7] Lascola, R. J., O'Rourke, P. E., Immel, D. M., & Larsen, E. (2021). *H-Canyon dissolver offgas monitoring using raman spectroscopy* (SRNL-STI-2021-00451). Savannah River National Laboratory

[8] Benton, A. F., & Elgin, J. C. (1926). The catalytic synthesis of water vapor in contact with metallic silver. *Journal of the American Chemical Society, 48*, 3027-3046.

[9] Hohmeyer, J., Kondratenko, E. V., Bron, M., Krohnert, J., Jentoft, F. C., Schlogl, R., & Claus, P. (2010). Activation of dihydrogen on supported and unsupported silver catalysts. *Journal of Catalysis, 269*, 5-14.

[10] Mohammad, A. B., Yudanov, I. V., Lim, K. H., Neyman, K. M., & Rosch, N. (2008). Hydrogen activation on silver: a computational study on surface and subsurface oxygen species. *The Journal of Physical Chemistry C, 112*, 1628-1635.

[11] Groves, M. C. E., & Sasonow, A. (2010). Uhde EnviNOx technology for NOX and N2O abatement: a contribution to reducing emissions from nitric acid plants. *Journal of Integrative Environmental Sciences, 7*(S1), 211-222.

[12] Sakaida, R. R., Rinker, R. G., Cuffel, R. F., & Corcoran, W., H. (1961). Determination of nitric oxide in a nitric oxide-nitrogen system by gas chromatography. *Analytical Chemistry, 33*(1), 32-34.

[13] Smith, R. H. (1967). *Procedure for coating berl saddles*. H-Canyon Reference Library

[14] Watkins, W. B. (1954). *Coating of 221F dissolver off-gas reactor packing with silver nitrate*. H-Canyon Reference Library

[15] Parkes, A. N. (1970). *Silver nitrate coating of unglazed ceramic berl saddles*. H-Canyon Reference Library

[16] Löffler, G., Wargadalam, V. J., Winter, F., & Hofbauer, H. (2000). Decomposition of nitrous oxide at medium temperatures. *Combustion and Flame, 120*(4), 427-438.

[17] Willis, C., Boyd, A. W., & Bindner, P. E. (1972). Primary yields and mechanisms in the radiolysis of N_2O from high intensity electron pulse irradiations of N_2O–O_2 mixtures. *Canadian Journal of Chemistry, 50*(10), 1557-1567.

[18] Zhao, G.-B., Hu, X., Argyle, M. D., & Radosz, M. (2004). N Atom radicals and $N_2(A^3\sum_u^+)$ found to be responsible for nitrogen oxides conversion in nonthermal nitrogen plasma. *Industrial & Engineering Chemistry Research, 43*(17), 5077-5088.

Supplementary Information

Catalytic Effects of Silver in Iodine Reactors for Dissolved Used Nuclear Fuel

Jarrod. M. Gogolski[a]*, Kathryn. M. L. Taylor-Pashow[a], Tracy. S. Rudisill[a], Michael L. Restivo[a], John M. Pareizs[a], Robert. J. Lascola[a], Patrick E. O'Rourke[a], and William. E. Daniel[a]

[a]*Savannah River National Laboratory, Aiken, SC, USA*

*E-mail: jarrod.gogolski@srnl.doe.gov

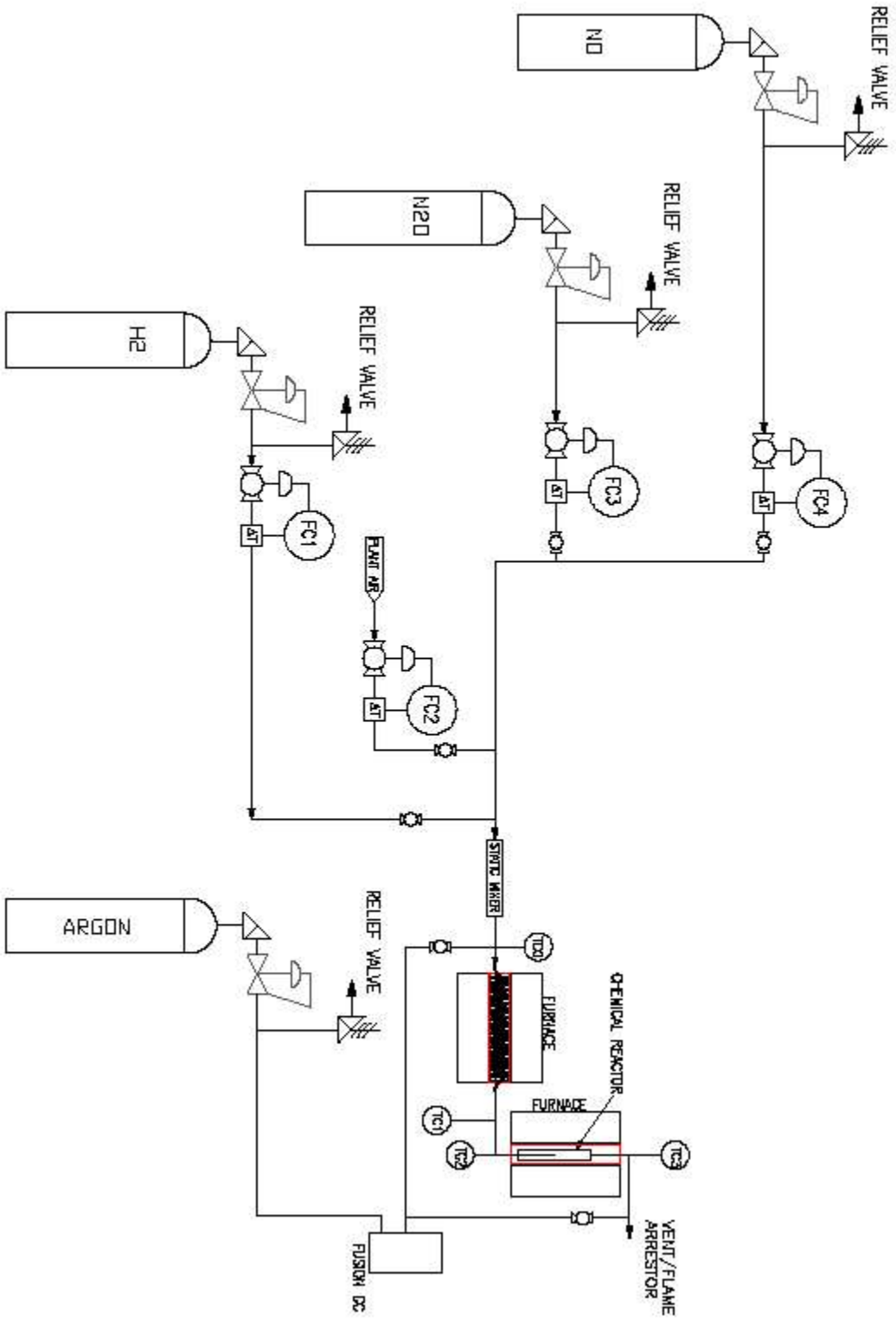

Supplementary Figure S1: Schematic diagram of the gas flow for the experimental equipment.

Supplemental Table SI: Initial (uncoated) and Final (silver nitrate-coated) Masses of Berl Saddles. Note: A similar batch size of uncoated berl saddles were dried over the same time to determine if the berl saddles were hydroscopic. The mass loss of 0.023% indicated that moisture absorption is minimal to negligible.

Batch	Initial Mass (g)	Final Mass (g)	Wt. % Change
1	28.5997	32.0158	11.9445
2	27.5931	31.4075	13.8238
3	29.1482	32.1538	10.3114
4	28.8199	31.3036	8.6180
5	29.6442	33.5563	13.1969
6	29.1685	32.4468	11.2392
7	29.307	32.6189	11.3007
8	28.8236	31.9622	10.8890
9	29.2791	32.5967	11.3310
10	29.3705	32.4993	10.6529
Average	**28.9754**	**32.2561**	**11.3307**

Residence Time Determinations

Adjusting the dissolver off-gas generation rate for the temperature increase at the iodine reactor results in a flow rate of 3.73 m^3/min at the reactor for the maximum off-gas case. The H-Canyon iodine reactor bed has a height of 2.50 m and a diameter of 0.60 m, resulting in an empty reactor volume of 0.70 m^3. The reactor is packed with 1.27 cm berl saddles resulting in a packed bed porosity of 60% or 0.42 m^3 of void volume [1]. Using the flow rate of 3.73 m^3/min through the void volume in the reactor results in a residence time of 7 seconds for the gas in the reactor. This residence time was used to determine the flow rate of gases needed to achieve the same residence time in the laboratory-scale reactor. Similar calculations were performed for the off-gas rates containing 1% and 1.9% H_2 and a summary of the results is provided in Table II of the main article. In addition, the residence times were varied from 0.5X to approximately 5X of the calculated residence time within the limits of achievable gas flows with the mass flow controllers used.

Supplementary Table SII. Test Matrix – Uncoated Berl Saddles.

Test ID	H_2 Vol.%	Residence Time (s)	Target Flow Rates (mL/min)				Cumulative Flow Rate (L/min)
			Air	N_2O	NO	H_2	
1A-UC	1.0	10.3 (1X)	257	17.3	55.2	3.32	0.33
1C-UC	1.0	48.9 (4.75X)	54.0	3.64	11.6	0.700	0.07
2A-UC	1.9	8.44 (1X)	262	44.5	90.2	7.69	0.40
2C-UC	1.9	40.9 (4.85X)	54.1	9.18	18.6	1.59	0.08
3A-UC	2.8	10.1 (1.5X)	173	46.0	110	9.48	0.34
3B-UC	2.8	32.0 (4.75X)	54.5	14.5	34.8	2.99	0.11

Supplementary Table SIII. Test Matrix – Silver Nitrate Coated Berl Saddles.

Test ID	H_2 Vol.%	Residence Time (s)	Target Flow Rates (mL/min)				Cumulative Flow Rate (L/min)
			Air	N_2O	NO	H_2	
1A-C	1.0	10.3 (1X)	257	17.3	55.2	3.32	0.33
1B-C	1.0	20.6 (2X)	128	8.64	27.6	1.66	0.17
1C-C	1.0	48.9 (4.75X)	54.0	3.64	11.6	0.700	0.07
1D-C	1.0	5.14 (0.5X)	513	34.6	110	6.65	0.66
2A-C	1.9	8.44 (1X)	262	44.5	90.2	7.69	0.40
2B-C	1.9	16.9 (2X)	131	22.3	45.1	3.84	0.20
2C-C	1.9	40.9 (4.85X)	54.1	9.18	18.6	1.59	0.08
3A-C	2.8	10.1 (1.5X)	173	46.0	110	9.48	0.34
3B-C	2.8	32.0 (4.75X)	54.5	14.5	34.8	2.99	0.11
4A-C	1.0	10.3 (1X)	329	0	0	3.32	0.33
4B-C	1.0	20.6 (2X)	165	0	0	1.66	0.17
4C-C	1.0	51.4 (5X)	65.8	0	0	0.665	0.07
4D-C	1.0	5.14 (0.5X)	658	0	0	6.65	0.66
5A-C	1.9	8.44 (1X)	397	0	0	7.69	0.40
5B-C	1.9	16.9 (2X)	198	0	0	3.84	0.20
5C-C	1.9	42.2 (5X)	79.4	0	0	1.54	0.08

Supplementary Table SIV. Experimental Conditions for Experiment 1.

Test ID	Berl Saddles	Input/ Output	Avg. Bed Temp. (°C)	Avg. H_2 Flow Rate (mL/min)	Avg. Air Flow Rate (mL/min)	Avg. N_2O Flow Rate (mL/min)	Avg. NO Flow Rate (mL/min)
1A-UC	uncoated	Input	176.2 (0.04%RSD)	3.31 (0.12%RSD)	245 (0.60%RSD)	17.2 (1.49%RSD)	55.1 (0.39%RSD)
1A-UC	uncoated	Output	172.4 (0.32%RSD)	3.31 (0.16%RSD)	245 (0.60%RSD)	17.1 (0.94%RSD)	55.0 (0.32%RSD)
1C-UC	uncoated	Input	176.9 (0.03%RSD)	0.686 (0.55%RSD)	50.5 (2.92%RSD)	3.28 (4.95%RSD)	11.9 (0.00%RSD)
1C-UC	uncoated	Output	177.1 (0.13%RSD)	0.687 (0.00%RSD)	51.5 (4.57%RSD)	3.26 (5.85%RSD)	11.9 (0.00%RSD)
1A-C	Silver coated	Input	181.1 (0.05%RSD)	3.32 (0.15%RSD)	256 (0.69%RSD)	17.3 (0.38%RSD)	55.4 (0.00%RSD)
1A-C	Silver coated	Output	180.1 (0.10%RSD)	3.32 (0.15%RSD)	256 (0.84%RSD)	17.3 (0.24%RSD)	55.4 (0.00%RSD)
1B-C	Silver coated	Input	182.3 (0.04%RSD)	1.68 (0.26%RSD)	125 (1.26%RSD)	8.63 (0.42%RSD)	27.6 (0.78%RSD)
1B-C	Silver coated	Output	181.9 (0.03%RSD)	1.67 (0.30%RSD)	125 (1.20%RSD)	8.64 (0.38%RSD)	27.7 (0.54%RSD)
1C-C	Silver coated	Input	181.8 (0.08%RSD)	0.71 (0.50%RSD)	55.0 (0.00%RSD)	3.65 (0.99%RSD)	11.5 (2.04%RSD)
1C-C	Silver coated	Output	182.6 (0.08%RSD)	0.71 (0.00%RSD)	55.5 (2.65%RSD)	3.65 (0.96%RSD)	11.5 (2.04%RSD)
1D-C	Silver coated	Input	179.4 (0.17%RSD)	6.66 (0.08%RSD)	518 (0.49%RSD)	34.6 (0.13%RSD)	110 (0.13%RSD)
1D-C	Silver coated	Output	178.8 (0.03%RSD)	6.66 (0.07%RSD)	517 (0.49%RSD)	34.6 (0.12%RSD)	110 (0.10%RSD)

Supplementary Table SV. Experimental Conditions for Experiment 2.

Test ID	Berl Saddles	Input/ Output	Avg. Bed Temp. (°C)	Avg. H_2 Flow Rate (mL/min)	Avg. Air Flow Rate (mL/min)	Avg. N_2O Flow Rate (mL/min)	Avg. NO Flow Rate (mL/min)
2A-UC	uncoated	Input	175.7 (0.02%RSD)	7.74 (0.06%RSD)	263 (0.92%RSD)	44.4 (0.26%RSD)	90.0 (0.19%RSD)
2A-UC	uncoated	Output	174.6 (0.34%RSD)	7.74 (0.06%RSD)	264 (0.86%RSD)	44.4 (0.29%RSD)	90.0 (0.24%RSD)
2C-UC	uncoated	Input	177.5 (0.11%RSD)	1.56 (0.25%RSD)	52.3 (4.87%RSD)	9.07 (1.14%RSD)	18.5 (1.22%RSD)
2C-UC	uncoated	Output	178.0 (0.02%RSD)	1.56 (0.27%RSD)	50.2 (2.08%RSD)	9.07 (1.03%RSD)	18.5 (1.30%RSD)
2A-C	Silver coated	Input	181.7 (0.02%RSD)	7.70 (0.06%RSD)	267 (0.89%RSD)	44.5 (0.11%RSD)	90.6 (0.12%RSD)
2A-C	Silver coated	Output	181.7 (0.02%RSD)	7.70 (0.07%RSD)	267 (0.89%RSD)	44.5 (0.11%RSD)	90.6 (0.00%RSD)
2B-C	Silver coated	Input	182.2 (0.03%RSD)	3.83 (0.06%RSD)	125 (1.20%RSD)	22.3 (0.20%RSD)	45.3 (0.55%RSD)
2B-C	Silver coated	Output	182.5 (0.01%RSD)	3.83 (0.09%RSD)	125 (0.85%RSD)	22.3 (0.23%RSD)	45.4 (0.50%RSD)
2C-C	Silver coated	Input	183.1 (0.02%RSD)	1.58 (0.32%RSD)	55.0 (2.87%RSD)	9.15 (0.23%RSD)	18.7 (1.16%RSD)
2C-C	Silver coated	Output	182.6 (0.04%RSD)	1.58 (0.32%RSD)	54.8 (1.95%RSD)	9.13 (0.38%RSD)	18.7 (0.93%RSD)

Supplementary Table SVI. Experimental Conditions for Experiment 3.

Test ID	Berl Saddles	Input/ Output	Avg. Bed Temp. (°C)	Avg. H_2 Flow Rate (mL/min)	Avg. Air Flow Rate (mL/min)	Avg. N_2O Flow Rate (mL/min)	Avg. NO Flow Rate (mL/min)
3A-UC	uncoated	Input	176.1 (0.11%RSD)	9.53 (0.05%RSD)	169 (1.35%RSD)	46.2 (0.30%RSD)	110 (0.18%RSD)
3A-UC	uncoated	Output	176.3 (0.32%RSD)	9.44 (0.05%RSD)	173 (1.48%RSD)	46.0 (0.19%RSD)	110 (0.16%RSD)
3B-UC	uncoated	Input	176.4 (0.07%RSD)	2.98 (0.13%RSD)	51.8 (4.75%RSD)	14.4 (0.58%RSD)	34.7 (0.00%RSD)
3B-UC	uncoated	Output	176.2 (0.03%RSD)	2.98 (0.12%RSD)	50.5 (2.98%RSD)	14.4 (1.14%RSD)	34.7 (0.00%RSD)
3A-C	Silver coated	Input	180.6 (0.05%RSD)	9.50 (0.04%RSD)	176 (1.12%RSD)	46.1 (0.09%RSD)	110 (0.16%RSD)
3A-C	Silver coated	Output	181.4 (0.08%RSD)	9.49 (0.03%RSD)	175 (0.84%RSD)	46.0 (0.08%RSD)	110 (0.13%RSD)
3B-C	Silver coated	Input	182.6 (0.06%RSD)	2.98 (0.17%RSD)	55.0 (0.00%RSD)	14.5 (0.29%RSD)	34.8 (0.71%RSD)
3B-C	Silver coated	Output	182.6 (0.04%RSD)	2.98 (0.15%RSD)	55.5 (2.65%RSD)	14.5 (0.39%RSD)	34.8 (0.61%RSD)

Supplementary Table SVII. Experimental Conditions for Experiments 4 and 5.

Test ID	Berl Saddles	Input/ Output	Avg. Bed Temp. (°C)	Avg. H_2 Flow Rate (mL/min)	Avg. Air Flow Rate (mL/min)
4A-C	Silver coated	Input	176.9 (0.08%RSD)	3.31 (0.15%RSD)	327 (0.74%RSD)
4A-C	Silver coated	Output	176.8 (0.07%RSD)	3.31 (0.15%RSD)	328 (0.78%RSD)
4B-C	Silver coated	Input	178.2 (0.08%RSD)	1.66 (0.29%RSD)	166 (1.29%RSD)
4B-C	Silver coated	Output	178.7 (0.02%RSD)	1.66 (0.26%RSD)	166 (1.06%RSD)
4C-C	Silver coated	Input	179.2 (0.04%RSD)	0.667 (0.47%RSD)	61.6 (3.87%RSD)
4C-C	Silver coated	Output	179.5 (0.02%RSD)	0.667 (0.32%RSD)	60.9 (3.24%RSD)
4D-C	Silver coated	Input	176.4 (0.23%RSD)	6.66 (0.05%RSD)	658 (0.38%RSD)
4D-C	Silver coated	Output	174.6 (0.13%RSD)	6.66 (0.08%RSD)	658 (0.39%RSD)
5A-C	Silver coated	Input	176.3 (0.15%RSD)	7.69 (0.07%RSD)	398 (0.64%RSD)
5A-C	Silver coated	Output	177.2 (0.04%RSD)	7.69 (0.06%RSD)	397 (0.64%RSD)
5B-C	Silver coated	Input	178.4 (0.06%RSD)	3.84 (0.13%RSD)	196 (1.01%RSD)
5B-C	Silver coated	Output	178.9 (0.03%RSD)	3.84 (0.11%RSD)	196 (0.90%RSD)
5C-C	Silver coated	Input	179.1 (0.02%RSD)	1.53 (0.32%RSD)	80.9 (2.44%RSD)
5C-C	Silver coated	Output	179.1 (0.03%RSD)	1.53 (0.30%RSD)	80.7 (2.18%RSD)

[1] Peters, M. S., & Timmerhaus, K. D. (1980). *Plant design and economics for chemical engineers* (3rd ed.). New York: McGraw-Hill Book Company.